On Measuring Closed-loop Nonlinearity – A Vinnicombe Metric Approach

Guan Tien Tan,
Dept. of Chem. & Bio. Eng.
University of British Columbia
guantien@chml.ubc.ca

Mihai Huzmezan,
Dept. of Elec. & Comp. Eng.
University of British Columbia
huzmezan@ece.ubc.ca

K. Ezra Kwok
Dept. of Chem. & Bio. Eng.
University of British Columbia
ezra@chml.ubc.ca

Abstract

The focal point of this paper is to develop a measure of closed-loop nonlinearity. In this work, the Vinnicombe metric and the Quasi-Linear Parameter Varying representation of a nonlinear system are exploited for this purpose. It is expected that the proposed measure can serve as a decision making tool for control engineers when considering whether a linear or a nonlinear control strategy should be employed to close the loop.

1 Introduction

Almost all processes are inherently nonlinear, however, this does not require the use of nonlinear control. For instance, [15] has shown that the control of a continuous stirred tank reactor (CSTR) temperature over a wide operating range can be achieved by using a single linear controller, in spite of its well known highly nonlinear behavior. Similar observations are also found in [4].

Feedback control normally employed to handle uncertainty, plant/model mismatch and noise attenuation, is also known to modify closed-loop nonlinearity. Measuring open-loop nonlinearity gives little information on the severity of closed-loop nonlinearity. Therefore, a systematic approach to quantify closed-loop nonlinearity is needed in order to check the adequacy of a linear controller before any attempts of using a nonlinear controller are made.

Over the past few decades, various linearity tests were proposed [1, 2, 3, 8, 12, 13]. However, most of them are measuring open-loop nonlinearity and are restricted to open-loop stable systems. Recently, several attempts have been made to tackle the quantification of closed-loop nonlinearity [4, 9]. Particularly, [4] proposes a measure based on the distance between a closed-loop containing a nonlinear process and a linear controller, and an ideal linear closed-loop. Albeit started independently, our approach is philosophically similar to that of [4]. In contrast to [4], the gap between the graphs (i.e. all bounded input-output pairs) of a nonlinear operator and its linear approximation is exploited in this work.

The gap metric framework has been first introduced to the control community by Zames and El-Sakkary [19] and later popularized by T.T. Georgiou and M.C. Smith, see [5, 6, 7]. The advantages of using the gap metric are that the resulting closed-loop nonlinearity measure is not restricted to any specific types of uncertainty representations such as additive or multiplicative, and it can handle open-loop unstable systems. In this work we show that when the nonlinear system can be approximated by a set of linear models representing the local dynamics of the systems at different operating points, the Vinnicombe (or ν-gap, denote by δ_ν) metric can be used to measure the closed-loop nonlinearity.

Since its debut, the ν-gap metric notion has attracted much attention particularly in robust control and system identification. Like the gap metric, the ν-gap metric measures the aperture of two closed Hilbert sub-spaces representing the graphs of two linear (possibly unbounded) operators. However, the strength of the ν-gap metric, as compared to the gap metric, lies in the fact that it gives the least conservative robust stability results whenever a homotopy condition is satisfied [16]. In this sense if the ν-gap between two plants is big, then a controller that gives satisfactory robust stability for one plant will show poor robust stability or even destablize the other plant. Likewise, if the ν-gap between two plants is small, then a controller which guarantees robust stability of one plant implies that it robustly stabilizes the other.

This work, assumes that the difference between a closed-loop containing a nonlinear plant and a unity feedback and an ideal linear closed-loop with a unity feedback is mainly due to closed-loop nonlinearity. This implies that these two closed-loops are subject to the same disturbances and noises injected at the same points in the loops. If the closed-loop nonlinearity (in gap terms, the uncertainty induced by the nonlinearity) is insignificant relative to what the best controller can cope with, then the closed-loop nonlinearity is said to be manageable by a linear controller. Otherwise, the closed-loop nonlinearity is significant, thus, the control design engineer might want to consider a nonlinear control strategy.

In this approach, the ν-gap metric is used to quantify the degree of closed-loop nonlinearity. To do so, the nonlinear plant is first decomposed into a set of linear models representing the nonlinear plant's local dynamics. Then the ν-gap metrics of all the possible pairs in the member set are computed. The best nominal model in the sense that it induces the smallest uncertainty ball is the one with the smallest ν-gap. The radius of this uncertainty ball is simply the maximum ν-gap in the member set. Since it is obvious that closed-loop nonlinearity not only depends on the plant itself, but also is a function of the controller, a linear controller is needed to assess the degree of nonlinearity. If the maximum ν-gap is smaller than what the best linear controller can cope with (which is typically measured in terms of the generalized stability margin), then this controller is claimed to maintain the closed-loop stability of the nonlinear plant. This means, in other words, that the closed-loop nonlinearity is manageable by a linear controller. Of course any statements about performance would be still conservative. Note that, at the best of authors' knowledge, none of the metrics mentioned above are exploited to provide a reliable closed-loop nonlinearity measure, hence, the ν-gap metric is used here in a completely novel context.

A nonlinear model (or operator), which captures the system's nonlinearity, is crucial for the success of the proposed measure. In this light, the focal point of this paper is to develop an indirect closed-loop nonlinearity measure by exploiting the ν-gap metric notion and the special structure of systems which admit a Quasi-LPV transformation.

This paper is organized as follows. Section 2 starts with notations used in this paper followed by a brief review on the Quasi-LPV representation and some preliminary results on the Quasi-LPV coprime factorizations together with a brief introduction to the $\mathscr{H}_\infty$ loop-shaping controller design procedure for completeness. Next, the Quasi-LPV ν-gap metric and a computational algorithm are presented in Section 3. In Section 4, an example involving a missile control problem is used to illustrate the proposed measure. Finally, some concluding remarks are drawn in Section 5.

2 Notation and Preliminaries

The notation used in this paper is standard: $\mathscr{L}_2$ is the finite energy signal space and $\mathscr{L}_2^+$ denotes signals in $\mathscr{L}_2[0,\infty)$. $G^*(s) = G^T(-s)$. $\bar{\sigma}(\cdot)$ and *wno* denote the maximum singular value and winding number, respectively. The scheduling parameter space is denoted by by Ω. In this sense, $\mathcal{S}_\Omega$ denotes all causal, $\mathcal{Q}_e$ stable, finite-dimensional Quasi-LPV systems defined in Ω. $\mathcal{S}_\Omega^-$ represents the elements in $\mathcal{S}_\Omega$ that have causal inverses. $[P,C]$ denotes the standard closed-loop containing the plant P and the controller C.

2.1 Quasi-LPV Transformation

Any plant exhibiting an output nonlinearity such as the one in Eq.(1)

$$\frac{d}{dt}\begin{bmatrix}\rho\\ z\end{bmatrix} = \phi(\rho) + \begin{bmatrix}\tilde{A}(\rho)_{11} & \tilde{A}(\rho)_{12}\\ \tilde{A}(\rho)_{21} & \tilde{A}(\rho)_{22}\end{bmatrix}\begin{bmatrix}\rho\\ z\end{bmatrix} + \begin{bmatrix}\tilde{B}_1(\rho)\\ \tilde{B}_2(\rho)\end{bmatrix}u, \quad (1)$$

can be recast into a Quasi-LPV representation as shown in Eq.(2) provided that $z_{eq}(\rho)$ is differentiable with respect to the state scheduling parameter ρ:

$$\frac{d}{dt}\begin{bmatrix}\rho\\ z-z_{eq}(\rho)\end{bmatrix} = A(\rho)\begin{bmatrix}\rho\\ z-z_{eq}(\rho)\end{bmatrix} + B(\rho)\,\big(u-u_{eq}(\rho)\big) \quad (2)$$

where

$$A(\rho) = \begin{bmatrix}0 & \tilde{A}_{12}(\rho)\\ 0 & \tilde{A}_{22}(\rho)-\frac{dz_{eq}(\rho)}{d\rho}\tilde{A}_{12}(\rho)\end{bmatrix}$$

and

$$B(\rho) = \begin{bmatrix}\tilde{B}_1(\rho)\\ \tilde{B}_2(\rho)-\frac{dz_{eq}(\rho)}{d\rho}\tilde{B}_1(\rho)\end{bmatrix}$$

In the above, $z_{eq}(\rho)$ denotes a family of equilibrium points obtained by setting the derivatives in Eq.(1) to zero. Note that for plants that do not exhibit output nonlinearity, the Quasi-LPV representation can approximate the actual plant up to a first order approximation of all other states except the scheduling state.

In order to use Eq.(2) for control purposes, the state dependent $u_{eq}(\rho)$ needs to be known. Any incorrect estimation of $u_{eq}(\rho)$ may jeopardize the robust property of the closed-loop system. To avoid this problem, an integrator at the plant input, which stores the trim input value $u_{eq}(\rho)$, can be added as suggested in [14]. As a consequence Eq.(2) can be rewritten as follows:

$$\frac{d}{dt}\begin{bmatrix}\rho\\ z-z_{eq}(\rho)\\ u-u_{eq}(\rho)\end{bmatrix} = \hat{A}(\rho)\begin{bmatrix}\rho\\ z-z_{eq}(\rho)\\ u-u_{eq}(\rho)\end{bmatrix} + \begin{bmatrix}0\\0\\1\end{bmatrix}v \quad (3)$$

where

$$\hat{A}(\rho) = \begin{bmatrix}0 & \tilde{A}_{12}(\rho) & \tilde{B}_1(\rho)\\ 0 & \tilde{A}_{22}(\rho)-\frac{dz_{eq}(\rho)}{d\rho}\tilde{A}_{12}(\rho) & \tilde{B}_2(\rho)-\frac{dx_{eq}(\rho)}{d\rho}\tilde{B}_1(\rho)\\ 0 & -\frac{du_{eq}(\rho)}{d\rho}\tilde{A}_{12}(\rho) & -\frac{du_{eq}(\rho)}{d\rho}\tilde{B}_1(\rho)\end{bmatrix}$$

In this development, a Quasi-LPV [14] is an appealing candidate owing to the following reasons: (i) plant's nonlinearity can be captured by selecting appropriate scheduling parameters; (ii) it is not a linearized version of the nonlinear plant, instead it is derived through a state transformation; (iii) a family of local linear models can be easily obtained by merely freezing the scheduling parameters.

2.2 Quasi-LPV Coprime Factorizations

In the sequel, we will consider a Quasi-LPV system which has the following state-space realization

$$\begin{aligned}\dot{x}(t) &= A(\rho)x(t) + B(\rho)u(t)\\ y(t) &= C(\rho)x(t) + D(\rho)u(t)\end{aligned} \quad (4)$$

where $\rho \subseteq x(t)$ is the scheduling parameter residing in the scheduling space Ω.

Definition 1 (Extended Quadratic Stability). *For a dynamic system characterized by the following state-space equation*

$$\dot{x}(t) = A(\rho)x(t), \quad \rho \in \Omega \quad (5)$$

the system is said to be extended quadratic stable ($\mathcal{Q}_e$ stable) if there exists a real differentiable positive-definite matrix function $P(\rho) = P^T(\rho) > 0$ such that

$$\frac{d}{dt}P(\rho) + A(\rho)^T P(\rho) + P(\rho)A(\rho) < 0, \quad \forall \rho \in \Omega. \qquad (6)$$

Lemma 1. *Any $\mathcal{Q}_e$ stable system is exponentially stable, if $\exists$ constants $\alpha,\ \beta > 0$ such that*

$$\bar{\sigma}(\Phi_\rho(t,\tau)) \leq \alpha e^{-\beta(t-\tau)} \quad \forall \rho \in \Omega$$

where $\Phi_\rho(t,\tau)$ denotes the transition matrix for Eq.(5)

Proof. see [18, pg. 16] □

Definition 2 ($\mathcal{Q}_e$ stabilizable). *The Quasi-LPV system given in Eq.(5) is said to be $\mathcal{Q}_e$ stabilizable if $\exists$ a continuous matrix function $F(\rho)$, such that the following system is $\mathcal{Q}_e$ stable $\forall \rho \in \Omega$*

$$\dot{x}(t) = \{A(\rho) + B(\rho)F(\rho)\}x(t).$$

Definition 3 ($\mathcal{Q}_e$ detectable). *The Quasi-LPV system given in Eq.(5) is said to be $\mathcal{Q}_e$ detectable if $\exists$ a continuous matrix function $H(\rho)$, such that the following system is $\mathcal{Q}_e$ stable $\forall \rho \in \Omega$*

$$\dot{x}(t) = \{A(\rho) + H(\rho)C(\rho)\}x(t).$$

Lemma 2 (Quasi-LPV Coprime Factorizations). *Let P_ρ have a continuous, $\mathcal{Q}_e$ stabilizable and $\mathcal{Q}_e$ detectable state-space realization*

$$P_\rho := \left[\begin{array}{c|c} A(\rho) & B(\rho) \\ \hline C(\rho) & D(\rho) \end{array}\right].$$

Let $F(\rho)$ and $H(\rho)$ be continuous matrix functions such that $\dot{x}(t) = \{A(\rho) + B(\rho)F(\rho)\}x(t)$ and $\dot{x}(t) = \{A(\rho) + H(\rho)C(\rho)\}x(t)$ are $\mathcal{Q}_e$ stable $\forall \rho \in \Omega$ and define (dropping ρ dependence for notation simplicity)

$$\begin{bmatrix} N_\rho & \tilde{Y}_\rho \\ M_\rho & \tilde{X}_\rho \end{bmatrix} := \left[\begin{array}{c|cc} A+BF & B & -H \\ \hline C+DF & D & I \\ F & I & 0 \end{array}\right] \qquad (7)$$

$$\begin{bmatrix} X_\rho & Y_\rho \\ \tilde{M}_\rho & -\tilde{N}_\rho \end{bmatrix} := \left[\begin{array}{c|cc} A+HC & H & -(B+HD) \\ \hline F & 0 & I \\ C & I & -D \end{array}\right], \qquad (8)$$

then

$$\begin{bmatrix} X_\rho & Y_\rho \\ \tilde{M}_\rho & -\tilde{N}_\rho \end{bmatrix} \begin{bmatrix} N_\rho & \tilde{Y}_\rho \\ M_\rho & \tilde{X}_\rho \end{bmatrix} = I \qquad (9)$$

Proof. see [18, pg. 149] □

Definition 4 (Contractive right coprime factorization). *Let $N_\rho \in \mathcal{S}_\Omega$ and $M_\rho \in \mathcal{S}_\Omega^-$ have the same number of columns. The ordered pair $[N_\rho, M_\rho]$ represents a contractive right coprime factorization (crcf) of P_ρ over the ring $\mathcal{S}_\Omega$, if*

1. *$P_\rho = N_\rho M_\rho^{-1}$;*
2. *$\exists\ X_\rho, Y_\rho \in \mathcal{S}_\Omega$ such that $X_\rho N_\rho + Y_\rho M_\rho = I$;*
3. *$[N_\rho^T\ M_\rho^T]^T$ is a contraction in the following sense*

$$\sup_{\rho\in\Omega} \sup_{\{u \in \mathscr{L}_2^+ : \|u\|_2 \leq 1\}} \left\| \begin{bmatrix} N_\rho \\ M_\rho \end{bmatrix} u \right\| \leq 1 \qquad (10)$$

Definition 5. *Define the contractive right graph symbol $G_\rho : \mathscr{L}_2^+ \mapsto \mathscr{L}_2^+ \otimes \mathscr{L}_2^+$ of an LPV system P_ρ as follows*

$$G_\rho := \begin{bmatrix} N_\rho \\ M_\rho \end{bmatrix}, \qquad (11)$$

where $[N_\rho, M_\rho]$ is a crcf of P_ρ.

Remark 1: It is obvious that G_ρ generates the set of all stable input-output pairs of the LPV system P_ρ by allowing G_ρ to act on the whole of $\mathscr{L}_2^+$.

Theorem 1 (Quasi-LPV Graph). *Let P_ρ have a continuous, $\mathcal{Q}_e$ stabilizable and $\mathcal{Q}_e$ detectable realization, then a contractive right graph symbol of P_ρ is given by*

$$G_\rho := \left[\begin{array}{c|c} A+BF & BS^{-\frac{1}{2}} \\ \hline C+DF & DS^{-\frac{1}{2}} \\ F & S^{-\frac{1}{2}} \end{array}\right] \qquad (12)$$

where $F = -S^{-1}(B^T X_1 + D^T C)$, $S = I + D^T D$, $R = I + DD^T$ and X_1 is a solution of the generalized control Riccati inequality (GCRI)

$$\begin{aligned} \dot{X}_1 + (A - BS^{-1}D^TC)^T X_1 + X_1(A - BS^{-1}D^TC) \\ -X_1 BS^{-1}B^T X_1 + C^T R^{-1} C < 0 \qquad \forall \rho \in \Omega \end{aligned} \qquad (13)$$

Proof. see [18, pg. 150] □

Remark 2: The results as stated here are for right coprime fractorizations. The dual results are easily obtained for left coprime factorizations.

Remark 3: Analogous to [16], the Quasi-LPV graph in Eq.(12) is used in the next section to define the corresponding Quasi-LPV ν-gap metric.

2.3 $\mathscr{H}_\infty$ Loop-Shaping

Proposed by [10], the $\mathscr{H}_\infty$ loop-shaping controller design method is based on the $\mathscr{H}_\infty$ robust stabilization and classical loop-shaping technique. The $\mathscr{H}_\infty$ loop-shaping consists of two major steps:

1. The open-loop plant is shaped using pre- and post-compensators to give a desired open-loop shape. Normally, it is desirable to shape the plant such that the maximum singular value frequency plot has a -20dB/decade slope at the crossover frequency.

2. Denoted by $P_s = W_2 P W_1$, the shaped plant is then robustly stabilized with respect to coprime factor uncertainty using a controller synthesis method based on an $\mathscr{H}_\infty$ optimization.

It is noted that the $\mathscr{H}_\infty$ norm of the closed-loop transfer function is minimized in the above $\mathscr{H}_\infty$ robust stabilization synthesis. Denoted by $b_{P,C}$, the reciprocal of Eq. (14) is often called the generalized stability margin which has a close relationship with the ν-gap metric. Mathematically, the genralized stability margin is defined as:

$$b_{P,C} := \begin{cases} \left\| \begin{bmatrix} P \\ I \end{bmatrix} (I-CP)^{-1} \begin{bmatrix} -C & I \end{bmatrix} \right\|_\infty^{-1}, \text{if } \begin{bmatrix} I & P \\ C & I \end{bmatrix}^{-1} \in \mathscr{H}_\infty \\ 0, \text{otherwise.} \end{cases} \tag{14}$$

For a more detail treatment of the $\mathscr{H}_\infty$ loop-shaping, see [10].

3 Main Results

Having defined the Quasi-LPV coprime factorizations, the Quasi-LPV ν-gap metric can be defined as follows:

Definition 6 (The Quasi-LPV ν-gap Metric). *The Quasi-LPV ν-gap δ_ν^{QLPV} is given by*

$$\delta_\nu^{QLPV}(P(\rho_i),P(\rho_j)) := \begin{cases} \|\tilde{G}_{\rho_j} G_{\rho_i}\|_\infty & \text{if } det(G^*_{\rho_j} G_{\rho_i})(j\omega) \neq 0 \\ & \forall \omega \in (-\infty, \infty) \text{ and} \\ & \text{wno } det(G^*_{\rho_j} G_{\rho_i})(j\omega) \\ & = 0, \ \forall \rho_i, \rho_j \in \Omega \\ 1 & \text{otherwise} \end{cases}$$

where G_{ρ_i} and $\tilde{G}_{\rho_j}$ denote the normalized right graph symbol of $P(\rho_i)$ and the normalized left graph symbol of $P(\rho_j)$, respectively as defined in Theorem 1. It is obvious that the $\delta_\nu^{QLPV} = \delta_\nu$ whenever ρ_i, ρ_j are frozen. Together with the $b_{P,C}$, the following theorem is one of the main results arising from the ν-gap metric notion.

Theorem 2. *Given a nominal plant $P(\rho_i) \in P_\rho$ obtained by freezing the scheduling parameter $\rho_i \in \Omega$, a controller C and a constant γ, then: $[P(\rho_j), C]$ is stable for all plants $P(\rho_j)$, $\forall \rho_j \in \Omega$ satisfying $\delta_\nu^{QLPV}(P(\rho_i), P(\rho_j)) \leq \gamma$ iff $b_{P(\rho_i),C} > \gamma$.*

Proof. Since $\delta_\nu^{QLPV} = \delta_\nu$ whenever ρ_i, ρ_j are frozen, the proof follows from that of [16], Theorem 4.5. □

Theorem 3. *Given a nominal plant $P(\rho_i) \in P_\rho$ and perturbed plants $P(\rho_j) \in P_\rho$ $\forall \rho_j \in \Omega$ obtained by freezing the scheduling parameter at $\rho_i, \rho_j \in \Omega$ respectively and a constant $\gamma < \sup_C b_{P(\rho_i),C}$, then: $[P(\rho_j), C]$ is stable for all controllers, C, satisfying $b_{P(\rho_i),C} > \gamma$ iff $\delta_\nu^{QLPV}(P(\rho_i), P(\rho_j)) \leq \gamma \ \forall \rho_j \in \Omega$.*

Proof. See [16], Theorem 4.5. □

The novel computational algorithm for closed-loop nonlinearity

1. Recast the nonlinear system into a Quasi-LPV form and grid the scheduling parameter space. A set of linear models is obtained by freezing the scheduling parameter.
2. For each model, the ν-gaps to all other models are obtained. $\delta_i = \{\delta_\nu^{QLPV}(P(\rho_i), P(\rho_j)), \ \forall \ \rho_j \in \Omega\}$.
3. Denote by L^*, the best nominal model for closed-loop control is the one that has the smallest ∞-norm in $\delta_i, \ \forall \ i$.
4. Apply pre- and post-compensators to L^*. ($L_s = W_2 L^* W_1$). Repeat step 2, but applying W_1 and W_2 to all $P(\rho_i)$ and $P(\rho_j)$ this time. Obtain the new L^* according to step 3 and subsequently the new L_s.
5. Design a robust controller using $\mathscr{H}_\infty$ loop-shaping for L_s and compute $b_{PC,\max}$, the maximum uncertainty ball that the linear controller can tolerate.
6. Find the farthest point L' (in the ν gap metric sense) in the polytope centered at L^*. The ν-gap between L^* and L' is denoted by δ'.
7. By empolying Theorem 2, the closed-loop nonlinearity is manageable by the designed linear controller if $b_{PC,\max} > \delta'$.
8. By using Theorem 3, the closed-loop nonlinearity is larger than what the linear controller can cope with if $b_{PC,\max} < \delta'$.

4 A Missile Control Problem

A missile control problem is used to illustrate the effectiveness of the proposed nonlinearity measure. The model is adopted from [14]. The control objective is to control normal accelaration, n_Z, by manipulating tail fin deflections. To achieve this, two control loops, namely an inner-loop and an outer-loop, are normally used. The inner-loop is responsible for controlling the angle of attack, α, using fin deflections, δ, while the outer-loop is used to control the n_Z by providing appropriate setpoints for α. However, since our main concern is on closed-loop nonlinearity measure, only the inner-loop design is considered here.

The Quasi-LPV representation of the missile dynamics is given as follows (see [14] for the model description and simulation parameters):

$$\frac{d}{dt}\begin{bmatrix} \alpha \\ q-q_{eq}(\alpha) \\ \delta-\delta_{eq}(\alpha) \end{bmatrix} = A(\alpha)\begin{bmatrix} \alpha \\ q-q_{eq}(\alpha) \\ \delta-\delta_{eq}(\alpha) \end{bmatrix} + \begin{bmatrix} 0 \\ 0 \\ 1 \end{bmatrix} v \tag{15}$$

where

$$A(\alpha) = \begin{bmatrix} 0 & 1 & \frac{fgQS\cos(\alpha/f)b_z}{WV} \\ 0 & -\frac{dq_{eq}(\alpha)}{d\alpha} & \frac{fQSdb_m}{I_{yy}} - \frac{dq_{eq}(\alpha)}{d\alpha}\frac{fgQS\cos(\alpha/f)b_z}{WV} \\ 0 & -\frac{d\delta_{eq}(\alpha)}{d\alpha} & -\frac{d\delta_{eq}(\alpha)}{d\alpha}\frac{fgQS\cos(\alpha/f)b_z}{WV} \end{bmatrix}$$

$$n_Z - n_{Z,eq} = \frac{QSb_Z}{W}(\delta - \delta_{eq}) \tag{16}$$

By using 50 grid points on the scheduling parameter α, Figure 1 shows the unshaped ν-gap contour between a chosen nominal model at α_i and all other models at $\alpha_j \in \Omega$. It is interesting to note that the contour is symmetric over the x-axis and the two nominal models at ± 8.75 are in fact identical. The best linear approximations, L^*, are those at $\alpha_i = \pm 8.75°$. Denote by L', the most dissimilar models from L^* are the ones at $\alpha_j = 0°, \pm 30°$ and the corresponding ν-gaps are 0.94. This means that any controllers that give satisfactory stability of the nominal plant will likely to destabilize the resulting closed-loop as the scheduling parameter is approaching 0° or $\pm 30°$. In fact, no matter which nominal model is chosen, the corresponding unshaped ν-gap exceeds 0.9 at some points when the angle of attack is evolved around $\pm 30°$.

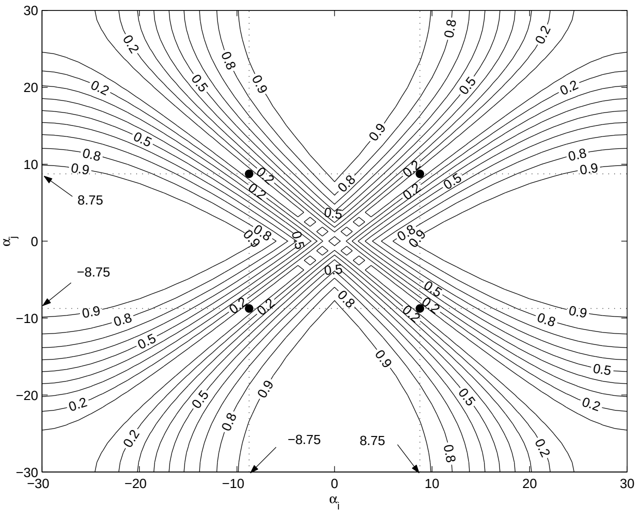

Figure 1: Unshaped ν gap contour

However, since the ν-gap is sensitive to dynamic scaling, an appropriate weighting of the nominal plant is required. This is done by employing the first step of the $\mathscr{H}_\infty$ loop-shaping technique. In this case, the corresponding pre- and post-compensators are:

$$W_1 = I_3 \text{ and } W_2 = \begin{bmatrix} \frac{58345(s+10)^2}{(s+300)(s+250)} & 0 & 0 \\ 0 & \frac{3(40s+400)}{s+100} & 0 \\ 0 & 0 & \frac{117000(s+10)}{(s+1)(s+200)} \end{bmatrix} \tag{17}$$

Figure 2 shows the resulting open-loop gain shapes.

Using the compensators in Eq.(17), the ν-gaps between a chosen nominal model and all other members in the scheduling space are recomputed. Figure 3 shows the corresponding shaped ν-gap contour. Clearly, there is a significant reduction in the ν-gap values, but the best linear models remain the same (i.e. the models at $\alpha_i = \pm 8.75°$). The most dissimilar models also remain the same, but the ν gap values are now 0.056, about 17 times less than that of the unshaped case. This implies that the weighted local models are very close to each other in closed-loop. The reduction in the ν-gap is due to the linearizing effect of feedback[3, 14].

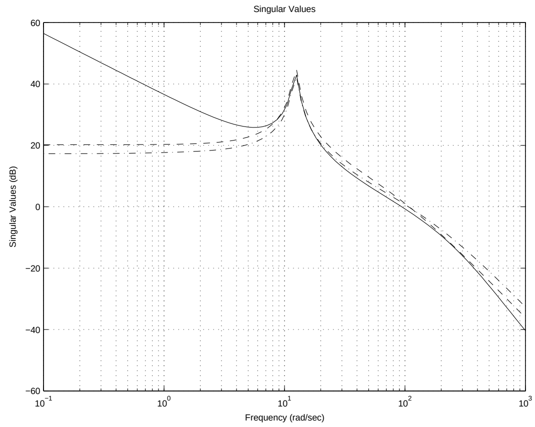

Figure 2: Shaped loop gains. Solid: α, dashed: $q - q_{eq}$, dashed-dotted: n_z

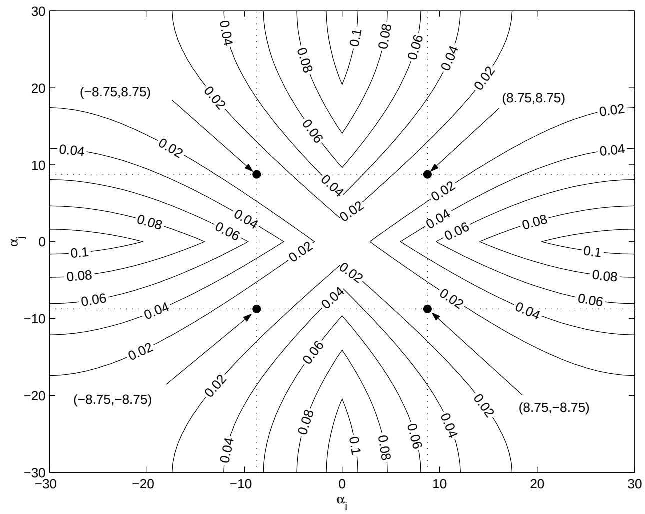

Figure 3: Shaped ν-gap contour

Based on the model at $\alpha_i = 8.75°$, the $\mathscr{H}_\infty$ linear controller with $b_{PC,\max} = 0.505$ is obtained via $\mathscr{H}_\infty$ loop-shaping technique. Since the worst ν-gap induced by the nonlinearity is less than the $b_{PC,\max}$ (i.e. $0.056 < 0.505$), Theorem 2 suggests that the designed controller is sufficient to cope with the closed-loop nonlinearity when the plant is pre- and post-compensated. Simulation results, as shown in Figure 4, confirm that the linear controller does provide good tracking performance when angle of attack α is evolving within the $\pm 30°$ available envelope.

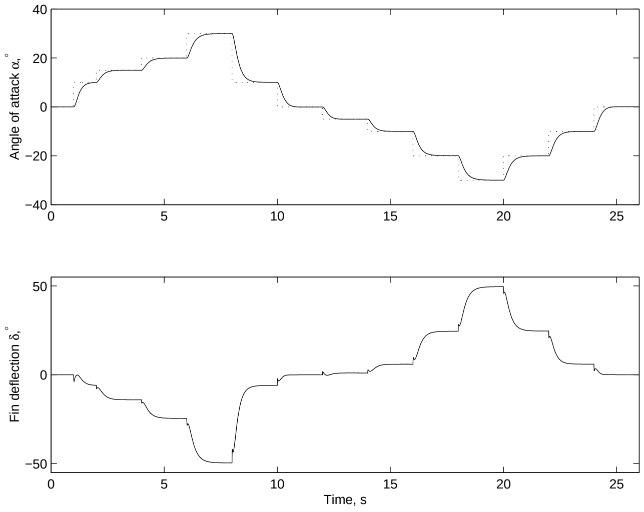

Figure 4: Servo responses of the angle of attack. (α achieved solid vs. α demanded dotted).

5 Conclusion

An indirect closed-loop nonlinearity measure using the ν-gap metric and the Quasi-LPV representation is proposed. The contribution of this work is two-fold. Firstly, it acts as an effective decision making tool for the control engineers when they are faced with the problem of deciding whether to stick to the linear control strategy or use a nonlinear control approach in solving their problems. Secondly, for a certain class of nonlinear systems, the proposed measure can be used as a way to design compensators which reduce the closed-loop nonlinearity. However, a systematic approach to closed-loop nonlinearity reduction needs a more indepth study. Dealing with non-differentiable nonlinearity such as hysteresis can be difficult. The proposed method can be extended to handle this type of nonlinearity by embedding such a nonlinearity using an integral quadratic constraints [11] followed by a Quasi-LPV transformation of the remaining model. This will be an extension of the work presented in [17].

References

[1] S.A. Billings and W.S.F. Voon. Structure detection and model validity tests in the identification of nonlinear systems. *IEEE Proceedings, Part D*, 130:193–199, 1983.

[2] W.A. Brock, W.D. Dechert, and J.A. Scheinkman. A test for independence based on the correlation dimension. Technical report, University of Wisconsin, Social Systems Research Institute, Madison, 1987.

[3] C.A. Desoer and Y.T. Wang. Foundations of feedback theory for nonlinear dynamical systems. *IEEE Trans. Circ. and Sys.*, 27:104–123, 1980.

[4] S.A. Eker and M. Nikolaou. Linear control of nonlinear systems: Interplay between nonlinearity and feedback. *AIChE Journal*, 48:1957–1980, 2002.

[5] T.T. Georgiou. On the computation of the gap metric. In *Proc. of the 27th Conf. on Decision and Control*, pages 1360–1361, 1988.

[6] T.T. Georgiou and M.C. Smith. Optimal robustness in the gap metric. *IEEE Trans. Automat. Contr.*, 35:673–686, 1990.

[7] T.T. Georgiou and M.C. Smith. Robustness analysis of nonlinear feedback systems: an input-output approach. *IEEE Trans. Automat. Contr.*, 42:1200–1221, 1997.

[8] M. Guay, P.J. McLellan, and D.W. Bacon. Measurement of nonlinearity in chemical process control systems: The steady-state map. *Can. J. Chem. Engng.*, 73:868–882, 1995.

[9] M. Guay, P.J. McLellan, and D.W. Bacon. Measurement of dynamic nonlinearity in chemical process control. In *Proceedings of ADCHEM 97*, Banff, Alberta, Canada, 1997.

[10] D. McFarlane and K. Glover. A loop shaping design procedure using $\mathscr{H}_\infty$ synthesis. *IEEE Trans. Automat. Contr.*, 37:759–769, 1992.

[11] A. Megretski and A. Rantzer. System analysis via integral quadratic constraints. *IEEE Trans. Automat. Contr.*, 42:819–830, 1997.

[12] M. Nikolaou. When is nonlinear dynamic modelling necessary? In *Proc. of the American Control Conf.*, San Francisco, CA, 1993.

[13] J.B. Ramsey. Test for specification errors in classical linear least squares regression analysis. *Journal of the Royal Statistical Society B*, 31:350–371, 1969.

[14] J. Shamma and J. Cloutier. Gain-scheduled missile autopilot design using linear parameter varying transformation. *Journal of Guidance, Control and Dynamics*, 16:256–263, 1993.

[15] G.T. Tan, M. Huzmezan, and E.K. Kwok. Vinnicombe metric as a nonlinearity measure. submitted to European Control Conference, 2003.

[16] G. Vinnicombe. Frequency domain uncertainty and the graph topology. *IEEE Trans. Automat. Contr.*, 38:1371–1383, 1993.

[17] G. Vinnicombe. On IQCs and the ν-gap metric. In *Proc. of the 37th IEEE Conf. on Decision and Control*, pages 1199–1200, 1998.

[18] G.D. Wood. *Control of Parameter-Dependent Mechanical Systems.* PhD thesis, University of Cambridge, 1995.

[19] G. Zames and A.K. El-Sakkary. Unstable systems and feedback: The gap metric. In *Proc. Allerton Conf.*, pages 380–385, 1980.